

## Exploring the stability of super heavy elements: First Measurement of the Fission Barrier of $^{254}\text{No}$

G. Henning<sup>1,2a</sup>, A. Lopez-Martens<sup>1,b</sup>, T.L. Khoo<sup>2</sup>, D. Seweryniak<sup>2</sup>, M. Alcorta<sup>2</sup>, M. Asai<sup>3</sup>, B. B. Back<sup>2</sup>, P. Bertone<sup>2</sup>, D. Boilley<sup>4</sup>, M. P. Carpenter<sup>2</sup>, C. J. Chiara<sup>2,5</sup>, P. Chowdhury<sup>6</sup>, B. Gall<sup>7</sup>, P. T. Greenlees<sup>8</sup>, G. Gurdal<sup>6</sup>, K. Hauschild<sup>1</sup>, A. Heinz<sup>9</sup>, C. R. Hoffman<sup>2</sup>, R. V. F. Janssens<sup>2</sup>, A. V. Karpov<sup>10</sup>, B. P. Kay<sup>2</sup>, F. G. Kondev<sup>2</sup>, S. Lakshmi<sup>6</sup>, T. Lauristen<sup>2</sup>, C. J. Lister<sup>6</sup>, E. A. McCutchan<sup>2</sup>, C. Nair<sup>2</sup>, J. Piot<sup>7c</sup>, D. Potterveld<sup>2</sup>, P. Reiter<sup>11</sup>, N. Rowley<sup>12</sup>, A. M. Rogers<sup>2</sup>, and S. Zhu<sup>2</sup>

<sup>1</sup>CSNS, IN2P3/CNRS and Université Paris Sud, France

<sup>2</sup>Argonne National Laboratory, USA

<sup>3</sup>Japan Atomic Energy Agency, Japan

<sup>4</sup>GANIL, CEA and IN2P3/CNRS and Normandie Université, France

<sup>5</sup>University of Maryland, USA

<sup>6</sup>University of Massachusetts Lowell, USA

<sup>7</sup>IPHC, IN2P3/CNRS and Université Louis Pasteur, France

<sup>8</sup>University of Jyväskylä, Finland

<sup>9</sup>Chalmers Tekniska Högskola, Sweden

<sup>10</sup>Flerov Laboratory of Nuclear Reactions, JINR, Russia

<sup>11</sup>Universität zu Köln, Germany

<sup>12</sup>IPN Orsay, IN2P3/CNRS and Université Paris Sud, France

**Abstract.** The gamma-ray multiplicity and total energy emitted by the heavy nucleus  $^{254}\text{No}$  have been measured at 2 different beam energies. From these measurements, the initial distributions of spin  $I$  and excitation energy  $E^*$  of  $^{254}\text{No}$  were constructed. The distributions display a saturation in excitation energy, which allows a direct determination of the fission barrier.  $^{254}\text{No}$  is the heaviest shell-stabilized nucleus with a measured fission barrier.

### 1 Introduction

The nucleus of interest  $^{254}\text{No}$  is situated at the very top of the chart of nuclides, in the region of the very heavy and super heavy elements. These nuclei are very special in that they are characterized by a decreasing and, for the heavier ones, a vanishing liquid drop fission barrier.

The reason why  $^{254}\text{No}$  does not fission with a very short lifetime [1] or why one has recently been able to synthesize and observe element 118 [2] is because of quantum-mechanical shell effects. Indeed, it is the gaps in the single-particle spectrum, which give additional binding to the nucleus and lower the ground state with respect to the liquid drop energy, thereby creating a barrier against fission.

<sup>a</sup>Current address: IPHC and Université Louis Pasteur, Strasbourg

<sup>b</sup>Corresponding author, e-mail: araceli.lopez-martens@csnsm.in2p3.fr

<sup>c</sup>Current address: GANIL

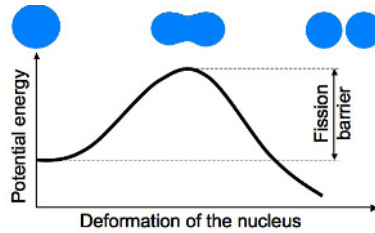


**Figure 1.** Schematic plot of the potential energy surface of the nucleus as a function of deformation, which shows the fission barrier and the associated shapes of the nucleus.

The height of the fission barrier  $B_f$  is defined as the energy difference between the saddle and the ground state energies (see Figure 1) and it is this barrier, which enables the existence of the heaviest elements. This makes it quite an interesting and valuable quantity to study.

## 2 Theoretical Predictions

Different models predict different barrier heights. So measuring  $B_f$  also provides a test of theories. In a microscopic-macroscopic description of  $^{254}\text{No}$  [3], the barrier height is predicted to be 6.7 MeV at 0 spin and the saddle is found to have a deformation parameter  $\epsilon=0.42$ , which corresponds to a superdeformed shape. Egido and Robledo used the Hartree-Fock Bogoliubov approximation with the Gogny force to calculate the evolution of the potential energy surface as a function of spin [4]. They obtain a larger saddle point deformation and a barrier height 2 MeV higher than the microscopic-macroscopic result. They also find that the barrier survives to quite high spins. Surprising as this may seem, this observation can be explained in terms of leading effects of angular momentum on the fission barrier [5]. For the nucleus to survive at high spins, what is important is the fractional change in moment of inertia between the saddle and the ground-state and for  $^{254}\text{No}$ , this change is predicted to be small since the saddle occurs at deformations only slightly greater than that of the ground-state.

## 3 Fission Barrier and Spin

How the barrier behaves as a function of spin, in other words the moment of inertia of the saddle-point configuration, is important to study because if the barrier were to disappear at a finite spin, we would not be able to make heavy elements. Indeed, one has to keep in mind that these heavy nuclei are produced in fusion-evaporation reactions, which bring in a substantial amount of angular momentum. The cross section to produce a given evaporation residue depends on 3 terms:

- (i) the probability that the colliding projectile and target will penetrate inside the entrance channel potential barrier and reach the contact point,
- (ii) the probability that this capture state evolves into a fused compound nucleus and finally
- (iii) the probability that the excited compound nucleus evaporates neutrons and decays to the ground-state of the nucleus of interest while surviving fission every step of the way.

This last term, called survival probability, reflects the competition between neutron emission, fission and gamma decay and one of the key parameters is the fission barrier, which enters into the fission width. A 2 MeV difference can affect the evaporation-residue cross-section by several orders of magnitude. In fact, by hindering the fission of the heated nucleus, the high fission barriers predicted around  $Z=114$  and  $N=184$  are thought to be responsible for the break in the trend of ever decreasing

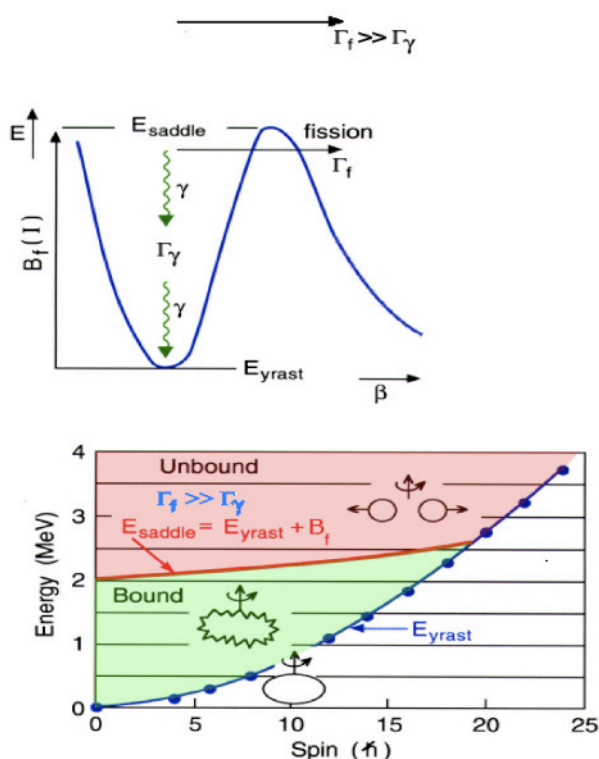


**Figure 2.** Cartoon showing how the competition between  $\gamma$  emission and fission splits the excitation energy vs spin plane into 2 regions. This feature is then exploited by the Entry Distribution Method to extract either a lower value or an absolute value of the height of the fission barrier (see text for details).

evaporation-residue cross sections as a function of evaporation-residue atomic number. Indeed, a significant increase in the total cross section of evaporation residues is observed starting at  $Z=112$ , with a maximum effect at  $Z=114-115$  [6].

Concerning the resilience of  $^{254}\text{No}$  to angular momentum, this was demonstrated by the pioneering work carried out at Argonne and Jyväskylä [7, 8], where the transitions of the ground-state rotational band were first observed. More recent work [9] has extended the ground-state band to spin  $24\hbar$ . These results already suggest that the fission barrier of  $^{254}\text{No}$  must still be quite substantial at high spin.

## 4 Experimental Fission Barriers

Experimentally, no fission barriers are known above Cf. The available data can be found in the RIPL2 library (<http://www-nds.iaea.org/RIPL-2/>). The probability to fission was measured in direct reactions on actinide targets [10] and by electromagnetic excitation of secondary beams following fragmentation reactions [11] and in a few cases, the EC delayed fission branch was used to determine the height of the fission barrier [12]. Unfortunately, these methods are not easily applicable (if at all) to the transfermium region. The first two methods cannot be used because of lack of suitable targets and

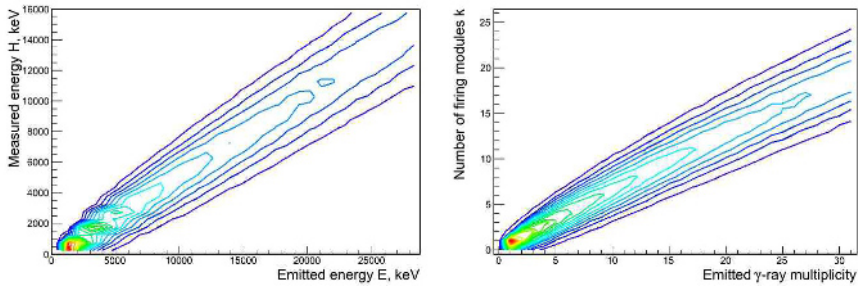


**Figure 3.** Measured energy response (left panel) and fold response (right panel) of GAMMASPHERE to the emission of a series of 898 keV gamma rays (see references [16–18] for details on the calibration method).

primary beams and the third method is limited to the cases where EC populates states around and above the fission barrier in the daughter nucleus.

## 5 The Entry Distribution Method

A new approach was proposed by P. Reiter more than 10 years ago now [13]. It is called the Entry Distribution Method and has the advantage that it is the only way to study the spin dependence of the barrier.

In the cases where the barrier lies below the neutron separation energy, fission is the dominant process above the barrier. This means that the excitation energy vs spin plane of Figure 2 is divided in 2 regions above the yrast line: The region above the saddle energy where fission dominates and the region below the saddle dominated by gamma decay. The method therefore consists in measuring the total excitation energy and spin of the nucleus of interest. Every point in the entry distribution is an event for which gamma decay wins over fission. If one puts enough energy into the system, one should observe that the distribution is limited by the fission process. The energy at which the distribution falls by 50% , called  $E_{1/2}$ , is related to the saddle energy. If the distribution is not limited, then the method allows to determine a lower limit for the fission barrier. If, on the other hand, enough energy is put into the system and the distribution is truncated, the absolute value of the fission barrier can be determined.

This method was applied to  $^{254}\text{No}$  by P. Reiter and collaborators [13].  $^{254}\text{No}$  was produced in the  $^{48}\text{Ca}$  on  $^{208}\text{Pb}$  reaction at 2 different energies. At 215 MeV bombarding energy, the measured entry distribution was found to be limited by the maximum energy available in the reaction. At 219 MeV, this was no longer the case and states up to  $22 \hbar$  and 6 MeV above the yrast line were populated. It was concluded that the barrier was at least 5 MeV high above  $10 \hbar$ . Another important conclusion is that the bulk of the cross section to produce  $^{254}\text{No}$  is at high spin.

## 6 Experimental Set-up

We recently repeated the experiment at 2 different bombarding energies: 219 MeV as in [13], and at higher energy; 223 MeV. The 10 pA  $^{48}\text{Ca}$  was delivered by the Argonne Tandem Linac Accelerator System.  $^{254}\text{No}$  was produced at the target position of the Fragment Mass Analyzer (FMA) [14], which separated the evaporation residues from the other unwanted reaction products.  $^{254}\text{No}$  was identified

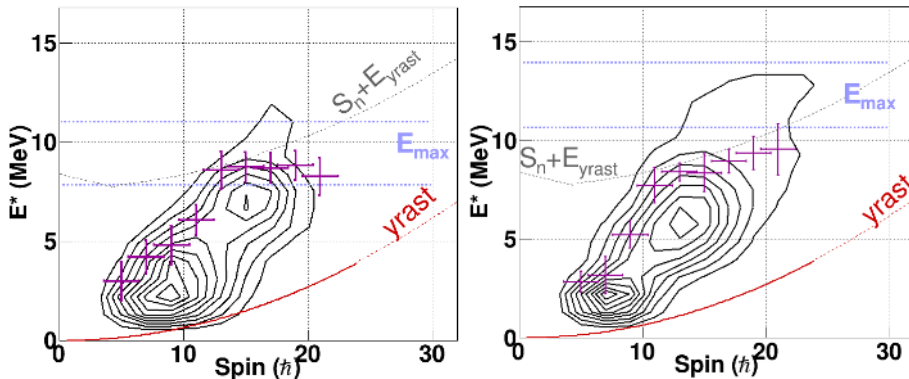


**Figure 4.** Measured entry distribution of  $^{254}\text{No}$  produced at 219 (left panel) and 223 (right panel) bombarding energies. The yrast line, neutron separation energy and limits of maximum energy allowed by the reaction are also indicated. The half-maximum  $E_{1/2}$  points are determined compared to the maximum of the energy distribution at the corresponding spin.

thanks to the combination of time of flight, position, energy loss and total energy information at the focal plane of the FMA. The gamma rays emitted by the excited  $^{254}\text{No}$  at the target position were detected by GAMMASPHERE [15], which was used in its calorimetric mode. This means that instead of using only the Ge part of GAMMASPHERE, which has  $\sim 10\%$  efficiency, we also used the BGO shields, which are composed of 6 lateral elements and a back plug. If we consider the Ge+BGO modules, then an efficiency of up to 78% efficiency can be reached. In our experiment, due to missing detectors and some timing issues, we measured an efficiency of 63%. The fold and energy responses of GAMMASPHERE measured with an  $^{88}\text{Y}$  source are shown in Figure 3.

During the experiment we measure the energy  $H$  detected in all the modules and the number  $k$  of firing modules. Then, using the energy and fold responses, we can obtain the distribution of emitted photon energy ( $E$ ) and multiplicity ( $M$ ) via the so-called unfolding procedure.

## 6.1 Unfolding Procedure

The unfolding is based on a Monte Carlo procedure [16–18] starting with an initial guess at the emitted ( $M, E$ ) distribution. This trial distribution is then passed through the measured response functions and compared to the measured distribution. In doing so, an improved guess at the true ( $M, E$ ) distribution can be made and the whole procedure can start again... This iterative procedure converges quite fast towards the final, best approximation of the ( $M, E$ ) distribution, which folds into the measured ( $k, H$ ) distribution.

To get to the total energy vs spin distribution, one has to know a little bit more about the nucleus of interest, in particular the contributions of conversion electrons to the total spin and energy. These parameters can be obtained and/or extracted from the known level scheme or from the experimental spectra. In the case of  $^{254}\text{No}$ , this was made possible by extensive prompt and decay spectroscopy studies [9, 19–22].

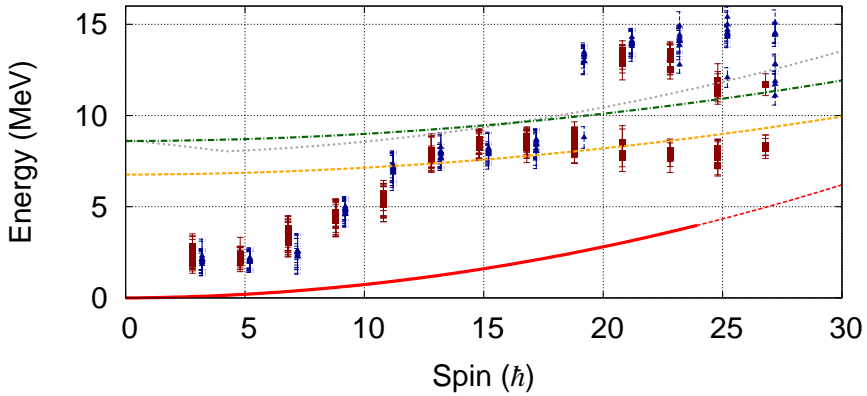


**Figure 5.** Saddle point energies extracted from the entry distributions measured at 219 MeV (red squares) and 223 MeV (blue triangles). Multiple unfolding results lead to multiple points per spin value. The black full line is the yrast energy, the dotted grey line represents the neutron separation energy. See text for more details.

## 6.2 Entry Distribution

The entry distributions obtained at 219 and 223 bombarding energies are shown in Figure 4. What is observed is that  $^{254}\text{No}$  can sustain more energy and spin at the higher bombarding energy. The averages go up by  $2 \hbar$  and 1 MeV respectively and the distribution extends beyond  $20 \hbar$ . This is at variance with the  $^{220}\text{Th}$  case, studied by Heinz et al. [23], and also in our experiment, which barely survives up to spin 20. This second experiment (with a different trigger compared to the Reiter et al. experiment [13]) confirms the fact that there is no significant population below  $5 \hbar$ . The purple crosses in Figure 4 represent the  $E_{1/2}$  points where the distribution falls to half its maximum value. They clearly show a saturation between 12 and  $25 \hbar$ , which can be attributed to the effect of fission depleting the gamma-emitting states. An absolute value of the fission barrier can therefore be determined for the first time in such a shell-stabilized heavy nucleus !

## 7 Results

If one plots the corresponding saddle energy,  $E_{saddle}$ , as a function of spin, one obtains the graph of Figure 5. The points at high spin (<5% of the population is above  $25 \hbar$ ) are discarded as they originate from (H,k) events resulting from random summing due to background, fission... From this plot, we can deduce that the saddle energy at  $14 \hbar$  is  $8.0 \pm 0.3$  MeV. Subtracting the energy of the yrast line at the same spin, one obtains the value of the fission barrier at  $14 \hbar$ :  $6.3 \pm 0.3$  MeV.

In green and orange are plotted the density functional and microscopic-macroscopic estimates, using a moment of inertia of  $140 \hbar^2/\text{MeV}$  (the Density Functional Theory value obtained from [4]). The microscopic-macroscopic estimate fits the data rather well.

One can fit the experimental saddle energies in the saturation region with the following spin dependent saddle expression:

$$E_{saddle}(I) = B_f(0) + \frac{\hbar^2}{2\mathcal{J}_{saddle}} I(I+1) \quad (1)$$

This cranking approximation is valid since higher order effects such as changes in the ground-state or saddle deformations, changes in the shell energy and pairing occur at higher angular momenta.

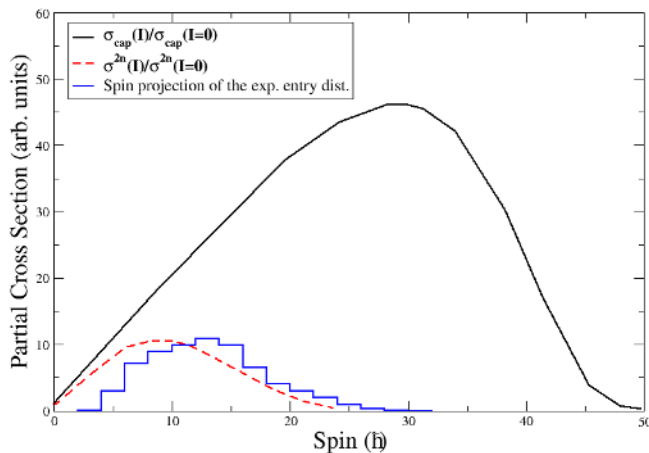


**Figure 6.** Theoretical partial capture cross section and spin distribution of  $^{254}\text{No}$  (taken from [24]). Our experimental spin distribution (in red) has been scaled for comparison.

Evidence for that is that  $^{254}\text{No}$  is a good rotor up to  $20 \hbar$  (the ground-state band moment of inertia changes by 10% from 0 to  $20 \hbar$  [9]). From the fit to the data using equation 1, one can extract a saddle moment of inertia of  $125 \pm 60 \hbar^2/\text{MeV}$  and a fission barrier at 0 spin of  $6.6 \pm 0.9 \text{ MeV}$ . Since the shell correction energy is of the order of 4 MeV [25, 26], one can say that shell effects account for 60% of the barrier. This is the opposite situation to  $^{220}\text{Th}$ , which we have studied in a similar fashion and where the fission barrier is dominated by the liquid drop term.

## 8 Conclusion and perspectives

This work represents the measurement of a fission barrier in the heaviest shell-stabilized nucleus. The entry distribution measurement, which allowed such a result to be obtained is also a sensitive probe of the reaction mechanism as it has revealed the dominance of high partial waves and a depletion of low partial waves as compared to theoretical expectations. This feature (visible in Figure 6) cannot be attributed to any triggering threshold as the only trigger used in the experiment was the detection of a recoil at the focal plane of the FMA, i.e no  $\gamma$  trigger was used. However, the multiplicity-to-spin conversion that is applied in the data analysis may not be adapted to low partial waves. This aspect clearly needs to be investigated further in a systematic way. In the near future, we will measure the entry distribution of an odd-Z nucleus:  $^{255}\text{Lr}$ . With the increased rate capability of digital GAMMAS-PHERE, we expect to be able to study the effect of not only the odd proton on the height of the fission barrier but also the stabilizing effect of the K quantum number.

## References

- [1] A. Ghiorso et al., Phys. Rev. Lett. **18** 401 (1967)
- [2] Y. Ts. Oganessian et al., Phys. Rev. C **74**, 044602 (2006)
- [3] P. Möller et al., Phys. Rev. C **79** 064304 (2009)
- [4] J.L.Egido and L.M. Robledo Phys. Rev. Lett. **85** (2000)

- [5] L.G. Moretto et al., Phys. Rev. C **67**, 017301 (2003)
- [6] Y. Oganessian, Nucl. Phys. News Vol. **23** 15 (2013)
- [7] P. Reiter et al., Phys. Rev. Lett. **82** 509 (1999)
- [8] M. Leino et al., Eur. Phys. J. A **6** 63(1999)
- [9] S. Eeckhaudt, P. Greenlees et al., Eur. Phys. J. A **26**, 227232 (2005)
- [10] B. B. Back et al., Phys. Rev. C **9** 1924 (1974) , B. Back et al., Phys. Rev. C **10** 1948 (1974)
- [11] A. Grewe et al. Nucl. Phys. A **614** 400 (1997)
- [12] D. Habs et. al. Z. Phys. A **285** 53 (1978)
- [13] P. Reiter et al., Phys. Rev. Lett. **84** 3542 (2000)
- [14] C. N. Davids et al., Nucl. Instrum. and Meth. B **70** 358 (1992)
- [15] I. Y. Lee, Nucl. Phys. **A 520** 641c (1990)
- [16] M. Jääskeläinen et al., Nucl. Instr. Meth. **204** 385 (1983)
- [17] P. Benet, PhD thesis, Université Louis Pasteur, Strasbourg (1988)
- [18] T. Lauritsen et al., Phys. Rev. C **75** (2007) 064309
- [19] R. Herzberg et al., Nature **442** 896 (2006)
- [20] S. Tandel et al., Phys. Rev. Lett. **97** 082502 (2006)
- [21] F. Hessberger et al., Eur. Phys. J. A **43** 5566 (2010)
- [22] R. Clark et al., Physics Letters B **690** 19 (2010)
- [23] A. Heinz et al., Nucl. Phys. A **682** 458 (2001)
- [24] V. I. Zagrebaev et al., Phys. Rev. C **65** 014607 (2001)
- [25] P. Möller et al., Atic Datat Nucl. Data Tables **59** 185 (1995)
- [26] M. Block et al., Nature **463** 785 (2010)